

Published in final edited form as:

Cancer Res. 2010 August 15; 70(16): 6609–6618. doi:10.1158/0008-5472.CAN-10-0622.

## Epigenetic silencing of miR-137 is an early event in colorectal carcinogenesis

Francesc Balaguer<sup>1,2</sup>, Alexander Link<sup>1,3</sup>, Juan Jose Lozano<sup>4</sup>, Miriam Cuatrecasas<sup>5</sup>, Takeshi Nagasaka<sup>6</sup>, C. Richard Boland<sup>1</sup>, and Ajay Goel<sup>1</sup>

<sup>1</sup> Department of Internal Medicine, Division of Gastroenterology, Charles A. Sammons Cancer Center and Baylor Research Institute, Baylor University Medical Center, Dallas, USA

<sup>2</sup> Department of Gastroenterology, Institut de Malalties Digestives i Metabòliques, Hospital Clínic, Centro de Investigación Biomédica en Red de Enfermedades Hepáticas y Digestivas (CIBEREHD), IDIBAPS, University of Barcelona, Barcelona, Catalonia, Spain

<sup>3</sup> Department of Gastroenterology, Hepatology and Infectious Diseases, Otto-von-Guericke University, Magdeburg, Germany

<sup>4</sup> Plataforma de Bioinformática, CIBEREHD, Barcelona, Catalonia, Spain

<sup>5</sup> Department of Pathology, Centre de Diagnòstic Biomèdic, Hospital Clínic, IDIBAPS, University of Barcelona, Barcelona, Catalonia, Spain

<sup>6</sup> Department of Gastroenterological Surgery and Surgical Oncology, Okayama University Graduate School of Medicine Dentistry and Pharmaceutical Sciences, Okayama, Japan

### Abstract

Global downregulation of microRNAs is a common feature in colorectal cancer (CRC). Whereas CpG island hypermethylation constitutes a mechanism for miRNA silencing, this field largely remains unexplored. Herein, we describe the epigenetic regulation of miR-137 and its contribution to colorectal carcinogenesis. We determined the methylation status of miR-137 CpG island in a panel of six CRC cell lines and 409 colorectal tissues (21 normal colonic mucosa from healthy individuals (N-N), 160 primary CRC tissues and their corresponding normal mucosa (N-C) and 68 adenomas). TaqMan RT-PCR and *in situ* hybridization were used to analyze miR-137 expression. *In vitro* functional analysis of miR-137 was performed. Gene targets of miR-137 were identified using a combination of bio-informatic and transcriptomic approaches. We experimentally validated the miRNA:mRNA interactions. Methylation of the miR-137 CpG island was a cancer-specific event, and was frequently observed in CRC cell lines (100%), adenomas (82.3%) and CRC (81.4%) but not in N-C (14.4%,  $p < 0.0001$  for CRC) and N-N (4.7%,  $p < 0.0001$  for CRC). Expression of miR-137 was restricted to the colonocytes in normal mucosa, and inversely correlated with the level of methylation. Transfection of miR-137 precursor in CRC cells significantly inhibited cell proliferation. Gene expression profiling after miR-137 transfection discovered novel potential mRNA targets. We validated the interaction between miR-137 and *LSD-1*. Our data firstly indicate that miR-137 acts as a tumor suppressor in the colon and is frequently silenced by promoter hypermethylation. Methylation-silencing of miR-137 in colorectal adenomas suggests it to be an early event, which has prognostic and therapeutic implications.

---

Address for correspondence: Ajay Goel, Ph.D. (ajay.goel@baylorhealth.edu) or C. Richard Boland, M.D. (rickbo@baylorhealth.edu), Gastrointestinal Cancer Research Laboratory, Baylor University Medical Center, 3500 Gaston Avenue, Suite H-250, Dallas, TX 75246, USA. Phone: 214-820-2692; Fax: 214-818-9292.

Conflict of interest: There is no conflict of interest to disclose for all authors.

## Keywords

microRNA; colorectal cancer; methylation; *LSD1*

---

## Introduction

microRNAs (miRNAs) are involved in the pathogenesis of multiple types of cancers, including CRC(1,2). Growing evidence suggests that miRNAs can act as oncogenes (*oncomiRs*) or tumor suppressor genes (*tsmiRs*), and they are involved in the early stages of carcinogenesis(2). The pattern of miRNA expression can be used to classify diverse types and subtypes of cancers(1,3), and miRNA expression profiles can have prognostic and therapeutic implications(4). Compared to mRNA, a modest number of miRNAs might be sufficient for clinical purposes, and more interestingly, miRNAs remain largely intact in different tissues and are virtually unaffected by RNA degradation(5). All these features make miRNAs a very exciting and promising tool for early tumor detection, prognostication, and treatment.

The causes of the widespread differential expression of miRNAs between tumor and normal cells are still unclear. Approximately 20% of all miRNAs are embedded within CpG islands and pharmacological unmasking of silenced miRNAs using epigenetic drugs have revealed that several miRNAs can be inactivated by this mechanism in CRC cell lines(6–8). These studies have permitted the identification of miRNAs that are methylation-silenced in CRC patients(7,9–11); however, the concept of epigenetic regulation of miRNAs in colorectal carcinogenesis remains largely unexplored..

miR-137 is one such miRNA, which is located on chromosome 1p22 within the non-protein coding RNA gene AK094607(12). This miRNA is embedded in a CpG island and is frequently silenced by methylation in several tumors(9,13,14). Ectopic transfection of the miR-137 precursor in oral cancer and glioblastoma multiforme inhibited cell growth, suggesting its tumor suppressive activity(13,14). However, the biological role of miR-137 as well as its specific downstream mRNA targets in colorectal carcinogenesis remains unknown. In addition, there is essentially no data about miR-137 disruption in adenomas, the precursor lesion of CRC. We have for the first time systematically characterized the role of miR-137 in the colon by addressing some of the issues mentioned above. We investigated the epigenetic regulation of miR-137 in a panel of six CRC cell lines and more than 400 colorectal tissues, which include both colorectal adenomas and cancers. We explored tumor suppressive features of miR-137 *in vitro*, and identified potential mRNA targets using whole genome expression profiling. In addition, we have successfully validated *LSD1*, a key element of the epigenetic machinery, as one of the targets of miR-137.

## Materials and Methods

### Cell lines and 5-aza-2-deoxy-cytidine treatment

We used six different CRC cell lines (HCT116, LoVo, RKO, SW48, HT29, SW480) obtained from the American Type Culture Collection (ATCC, Manassas, VA) during the last 2 years. In our lab, all cells are tested and authenticated every six months using known genetic and epigenetic marks. Cells were grown in appropriate culture conditions. For demethylation experiments, cells were treated with 2.5  $\mu\text{mol/L}$  5-aza-2-deoxy-cytidine (5-AZA; Sigma) for 72h, replacing the drug and medium every 24h.

## Tissue specimens

A collection of 409 colorectal tissues were analyzed in this study which included 113 sporadic primary CRCs with their corresponding adjacent normal colonic mucosa (N-C) and 68 colorectal adenomas obtained from the Okayama University Hospital, Okayama, Japan. Twenty-one normal colonic mucosa specimens from non-tumor patients (N-N) were collected at the Hospital Clinic of Barcelona, Spain. Additionally, 47 CRC tissues and the corresponding adjacent normal mucosa from 11 patients with Lynch syndrome, 14 patients with microsatellite unstable CRCs and 22 patients with microsatellite stable tumors were collected at Baylor University Medical Center, Dallas TX. All patients provided written informed consent and the study was approved by the Institutional Review Boards of all participating institutions. Clinico-pathological data of the patients is presented in Tables 1 and Supplementary table 1.

## RNA extraction

Total RNA extraction was undertaken using the miRVana RNA extraction kit (Ambion Inc, Austin, TX) and the RecoverAll kit (Ambion Inc, Austin, TX), according to the manufacturer's instructions.

## DNA methylation analysis

DNA methylation status of the miR-137 CpG island was established by PCR analysis of bisulfite modified genomic DNA (EZ DNA methylation Gold Kit, Zymo Research) using three different methodologies. First, methylation status was analyzed by bidirectional bisulfite sequencing of HCT116 and RKO cell lines. Secondly, we performed methylation specific PCR (MSP) using primers for either the methylated or unmethylated DNA in the six CRC cell lines used in the study. Finally, we used bisulfite pyrosequencing for quantitative methylation analysis (PSQ HS 96A pyrosequencing system, QIAGEN). The primers used are described in the Supplementary Table 2.

## Analysis of miRNA expression using TaqMan RT-PCR

Expression of mature miR-137 was analyzed using the TaqMan miRNA Assay (Applied Biosystems Inc., Foster City, CA). Expression of RNU6B (Applied Biosystems Inc., Foster City, CA) was used as an endogenous control. All the experiments were done in triplicate.

## *In situ* hybridization

The *in situ* detection of miR-137 was performed on 5- $\mu$ m FFPE sections from five normal colonic mucosa tissues, three adenomatous polyps, and five colorectal adenocarcinomas. Briefly, the slides were hybridized with 10 pmol probe (LNA-modified and DIG-labeled oligonucleotide; Exiqon) complementary to miR-137 and after incubation with anti-DIG-AP Fab fragments conjugated to alkaline phosphatase, and the hybridized probes were detected by applying nitroblue tetrazolium/5-bromo-4-chloro-3-indolyl phosphate color substrate (Roche) to the slides. Positive controls (RNU6B, Exiqon) and no probe controls were included for each hybridization procedure.

## Transfection of miR-137 precursor molecules

HCT116 cells were transfected with Pre-miR miRNA precursor molecules (Ambion Inc, Austin, TX) or Pre-miR miRNA negative control #1 (Ambion Inc, Austin, TX) at a final concentration of 100 nM, using Lipofectamine 2000 (Invitrogen, Rockville MD) according to manufacturer's instructions. For microarray and RT-PCR analysis, total RNA was extracted 48h after transfection; for Western blot analysis, cell lysates were prepared 48h after transfection. In order to ensure the transfection efficiency, we verified the protein downregulation of CDK6, a previously validated target by Western blotting.

## Gene expression microarray analysis, RT-PCR and miRNA target prediction

HCT116 cells were transfected with control miRNA precursor or miR-137 precursor as described above. Extracted RNA was amplified using Illumina's TotalPrep RNA Amplification Kit. RNA integrity was assessed using the Agilent 2100 Bioanalyzer. Labeled cRNA was hybridized overnight to Human HT-12 V3 chips, washed, and scanned on an Illumina BeadStation-500. Illumina's BeadStudio version 3.1 was used to process signal intensity values from the scans, and background subtracted. Normalization was done using quantiles with the Lumi R-package. Fold-changes were calculated with respect to their respective control. miRecords website (<http://mirecords.umn.edu/miRecords>)(15) was used to predict the miRNA targeting of miR-137. In order to narrow down the list of predicted targets, genes found to be downregulated (>2 fold-change) after transfection of miR-137 precursor in the microarray were crossed with the genes predicted to be targets based on miRecords. Genes previously found to be associated with either CRC specifically or carcinogenesis in general were selected for validation.

For reverse transcription-PCR (RT-PCR), RNA was reverse transcribed to cDNA from 1µg of total RNA using random hexamers and Advantage RT-for PCR Kit (Clontech Laboratories, CA). Power SYBR Green (Applied Biosystems Inc., Foster City, CA) RT-PCR was performed for selected targets found with the strategy described above. Results were normalized to the expression of  $\beta$ -actin. All the experiments were performed in triplicates. Primer sequences are listed in the Supplementary Table 2.

## Western blot analysis

Western blot analysis was carried out using standard methods. The following primary antibodies were used: anti-CDK6 (Cell Signaling, MA) at 1:2000 dilution; anti-LSD1 (Cell Signaling, MA) at 1:250 dilution; anti-SEMA4D (BD Transduction Laboratories, San Jose, CA) at 1:250 dilution; anti-AURKA (Cell Signaling, MA) at 1:250 dilution; anti-CSE1L (BD Transduction Laboratories, San Jose, CA); anti-BX1 (Cell Signaling, MA) at 1:1000 dilution; anti- $\beta$ -actin antibody (Clone AC-15) at 1:32000 dilution.

## Luciferase reporter assay

Luciferase constructs were made by ligating oligonucleotides containing the wild-type or mutant putative target site of the *LSD1* 3'-UTR downstream of the luciferase gene in the pMIR Reporter Luciferase vector (Ambion Inc, Austin, TX). Primers are detailed in Supplementary Table 2. Cells were co-transfected using Lipofectamine 2000 (Invitrogen, Rockville MD) with 400 ng of firefly luciferase reporter vector containing the wild-type or mutant oligonucleotides, 200 ng of pGal control vector (Ambion Inc, Austin, TX), and 50 pmol of either miR-137 or negative control precursor. The parental luciferase plasmid was also transfected as a control. Luciferase activity was measured 48h after transfection (Bright Glo Luciferase Assay System, Promega) using  $\beta$ -galactosidase for normalization (Beta-galactosidase Enzyme Assay System, Promega). Experiments were performed in triplicate in three independent experiments.

## Bromodeoxyuridine (BrdU) proliferation assay

The proliferation index was measured by BrdU incorporation in colon cancer cells 96h after transfection of either control miRNA precursor or miR-137 precursor as described above (Cell Proliferation ELISA, BrdU, Roche), following manufacturer's instructions. Experiments were performed in triplicate in three independent experiments.

## Statistical analysis

All data were analyzed using the SPSS 13 (Chicago, IL, USA) and Graph Pad Prism 4.0 (San Diego, CA) statistical software. Quantitative variables were analyzed using Student's test, Wilcoxon test (non-parametric paired analysis) and Mann-Whitney U test (non paired analysis). Qualitative variables were analyzed using either the Chi Square Test or the Fisher's test. A two sided p-value of  $< 0.05$  was regarded as significant.

## Results

### miR-137 is epigenetically silenced in CRC cell lines

To determine the DNA methylation status in the miR-137 CpG island we used a sequential approach. The CpG island of miR-137, along with the localization of PCR products for each approach, are represented in Figure 1A. First, we performed direct bisulfite sequencing of the promoter region of miR-137 in HCT116 and RKO cell lines, and we found extensive methylation throughout its promoter region in both cell lines, which was reversible following 5-AZA treatment (Figure 1C). Second, using MSP, we found that the miR-137 CpG island was extensively methylated in all of the CRC cell lines, and as expected, treatment with 5-AZA induced significant demethylation (Figure 1B). Third, we performed methylation analysis of miR-137 CpG island by quantitative pyrosequencing (Figures 1D and 2A). Methylation, when present, generally affected all four sites CpG sites homogeneously; thus, their average was taken as the final measurement for analysis. The average methylation levels in HCT116, LoVo, RKO, SW48, HT29 and SW480 cells were 83%, 28%, 79%, 73%, 79% and 29%, respectively.

We next analyzed the expression of miR-137 in the same panel of CRC cell lines using TaqMan RT-PCR, and we found an inverse correlation between the degree of CpG island methylation measured by pyrosequencing and the level of expression (Figure 2A and B). Along with demethylation, treatment with 5-AZA induced upregulation of miR-137 in CRC cell lines, suggesting that the expression of miR-137 is suppressed through CpG island promoter methylation in the majority of CRC cell lines.

### Epigenetic silencing of miR-137 is an early event in colorectal carcinogenesis

We next used the miR-137 pyrosequencing assay to analyze the methylation status in a cohort of colorectal cancer tissues which included 21 normal mucosa from non-tumor patients (N-N), 113 CRC tissues with their corresponding adjacent normal mucosa (N-C), and 68 colorectal adenomas. The mean level of methylation ( $\pm$ standard deviation, SD) in N-N, N-C, CRC and adenomas was 7.70% ( $\pm 4.18$ ), 10.27% ( $\pm 6.88$ ), 31.67% ( $\pm 17.25$ ) and 33.09% ( $\pm 21.06$ ), respectively (Figure 2C). Thus, the level of methylation was significantly higher in CRC tissues compared to their corresponding histologically normal mucosa (31.67% vs 10.27%,  $p < 0.0001$ ), demonstrating the cancer specificity of miR-137 methylation. In addition, the level of miR-137 methylation in N-N or N-C did not correlate with older age (data not shown). On the other hand, we observed a significantly higher degree of methylation in N-C compared to N-N (10.2% vs 7.7%,  $p = 0.0352$ ) consistent with the paradigm of methylation-related field defects in CRC. Finally, and more interestingly, methylation of miR-137 in adenomatous tissues showed the same degree of methylation as CRC tissues ( $p = 0.8352$ ), suggesting that methylation of this miRNA is an early event in colorectal carcinogenesis.

In order to determine whether miR-137 methylation might be different among the different molecular subtypes of CRC based on the presence of microsatellite instability (MSI), we next analyzed miR-137 methylation status in tumor and matching normal tissues (N-C) from 11 patients with Lynch syndrome, 14 patients with sporadic MSI, and 22 MSS patients. The

mean levels of methylation in Lynch, sporadic MSI and MSS were 22%, 27.3% and 24.7%. The corresponding levels in N-C were 6.4%, 6.2% and 7.3%, respectively. Accordingly, miR-137 methylation seems to be equally present in all molecular subtypes of CRC.

Since pyrosequencing analysis allows quantitative measurements, we next analyzed miR-137 methylation results as a categorical variable. We determined a methylation cut-off based on the average miR-137 methylation levels in normal mucosa from non-tumor individuals plus two standard deviations (cut-off:15%). Based upon these results, miR-137 was methylated in 4% (1/21) of N-N, 14.4% (16/111) of N-C, 81.4% (92/113) of CRC and 82.3% (56/68) of adenomas. Clinico-pathological features of CRC and adenomas patients are listed in Table 1 and Supplementary Table 1, respectively. Patients with CRC-associated miR-137 methylation were significantly older than those without methylation (66 vs 60 years-old,  $p=0.024$ ), showed more frequent somatic *KRAS* mutations (37% vs 14.3%,  $p=0.046$ ) and were less frequently associated to mucinous features (2.2% vs 15%,  $p=0.039$ ). There was no association between methylation status and TNM stage. In adenoma patients, we observed a significantly higher degree of methylation in villous compared to non-villous adenomas (44.28% vs 29.08%,  $p=0.0051$ ).

### miR-137 is constitutively expressed in the colonic epithelium and downregulated in CRC

We used TaqMan RT-PCR to assess the expression of miR-137 in 15 pairs of CRC and normal colonic mucosa, and found substantial downregulation of the expression in the tumor compared with the normal mucosa (Figure 2D). Interestingly, the only 2 cases that did not show downregulation in the tumor tissue were those not associated with methylation (data not shown).

To investigate which specific cell types expressed miR-137 in the colon, we performed *in situ* hybridization using 5'-DIG-labeled LNA probes, a technique that has been applied to the detection of miRNA *in situ* in FFPE tissues (Figure 3). In normal colonic mucosa, miR-137 was expressed only in the colonic epithelial cells throughout the colonic crypts. However, none of the adenomatous and CRC samples showed miR-137 expression, consistent with our observation that miR-137 is silenced in the majority of colonic neoplastic tissues.

### miR-137 transfection inhibits cell proliferation

Since we discovered that miR-137 is epigenetically silenced in CRC through CpG island methylation, we next performed functional studies to determine whether miR-137 had *in vitro* tumor suppressive features following transfection of miR-137 precursor into CRC cell lines. We performed BrDU incorporation assays after transfection of either miR-137 precursor or a negative control precursor in three different colon cancer cell lines. Restoration of miR-137 significantly reduced cell proliferation in HCT116 and RKO but not in SW480 (Figure 5D), suggesting the specificity of miR-137 as a tumor suppressor in CRC.

### Identification of potential gene targets of miR-137

In order to identify gene targets of miR-137, we first performed whole genome gene expression analysis in HCT116 cells after transfection of either miR-137 or negative control precursors. Four hundred ninety-one genes showed more than 2-fold decrease in their expression following miR-137 transfection, compared to the negative controls (Supplementary Table 3). We next used the miRecords resource(15) to obtain a list of predicted miR-137 targets. This bioinformatics approach integrates information of predicted miRNA targets produced by 11 established miRNA target prediction programs, thus providing a more accurate and comprehensive assessment of predicted targets compared to a single database. Selecting the predicted targets from at least 4 of the 11 prediction tools

included in the website, we obtained a list of 505 potential targets (Supplementary Table 3). After cross-referencing the list of miR-137-related gene targets from our own gene expression microarray data and information gathered from miRecords database, we determined that 32 genes met the criteria of down-regulation by miR-137 transfection and being an *in silico* predicted target (Figure 4A and B).

We first validated the microarray data by RT-PCR (Figure 4C) for a subset of selected genes. Lysine (K)-specific demethylase 1A (KDM1A, also known as *LSD1*), chromosome segregation 1-like (*CSE1L*), Y box binding protein 1 (*YBX1*), Semaphorin 4D (*SEMA4D*) and Aurora Kinase A (*AURKA*) were chosen for validation because of their putative role in carcinogenesis. Sequence interaction between the 3'UTR region of these genes and miR-137 is shown in Supplementary Figure 1. RT-PCR results were highly concordant with microarray data for all selected genes. All of these genes contain well conserved target sites in their 3'UTR region for miR-137 and western blot analysis effectively showed different degrees of downregulation of expression in 3 of 5 selected genes after miR-137 precursor transfection (Figure 4D).

### ***LSD1* is a direct target of miR-137**

We next explored the functional interaction between miR-137 and *LSD1* (Figure 5A-C). The expression level of miR-137 and *LSD1* mRNA were determined in 6 CRC cell lines by TaqMan RT-PCR and RT-PCR, respectively (Figure 5B). In CRC cell lines with lower endogenous miR-137 expression (HCT116, LoVo, RKO, SW48), a higher *LSD1* expression level was observed, whereas in HT29, the cell line with higher expression levels of miR137, the amount of *LSD1* was much lower.

To determine if the 3'UTR region of *LSD1* was indeed a functional target site of miR-137, a luciferase reporter plasmid harboring either the wild-type or mutated predicted region of interaction at the *LSD1* 3'UTR region was constructed. The transient transfection of HCT116 cells with the wild-type reporter plasmid and the miR-137 precursor led to a decrease of luciferase activity in comparison with the control precursor (Figure 5C). However, the luciferase activity remained unaffected following transfection with either the parental plasmid or the one with the mutated sequence.

## **Discussion**

In this study, we report that epigenetic silencing through promoter methylation of miR-137 is an early event in colorectal carcinogenesis. *In situ* hybridization analysis showed that this miRNA is constitutively expressed in the normal colonic epithelium and is silenced in neoplastic tissues. Gene expression analysis combined with *in silico* prediction tools allowed us to identify several potential targets of miR-137, including *LSD1*, a histone demethylase that plays a central role in the epigenetic machinery.

Our data indicate that methylation of the miR-137 promoter is an early event in colorectal carcinogenesis, supported by the fact that the average methylation level in adenomas was similar to CRC specimens (31.67% vs 33.09%, respectively;  $p=0.8352$ ). In addition, miR-137 methylation appears to be tumor-specific, since it preferentially occurs in neoplastic tissues and its methylation in normal colonic mucosa did not increase as a function of age. More interestingly, we found a higher degree of average methylation in histologically normal colorectal mucosa from CRC patients compared to the normal mucosa from non-tumor patients (10.27% vs 7.7%, respectively;  $p=0.0352$ ), consistent with the epigenetic field defect proposed in CRC(16). The rationale for this phenomenon relies on the fact that sporadic CRCs are thought to arise from a region of cells characterized by a "field defect"(17). DNA methylation of multiple genes has been proposed as a major

contributor to the field defect hypothesis (16), however, only two previous studies have suggested that miRNA methylation may have analogous manifestation in the gastrointestinal tract. Grady et al. found that miR-342, an intronic miRNA encoded within the *EVL* gene, was methylated in 56% of normal-appearing colonic mucosa from CRC patients and in six out of nine adenomas(10). In gastric cancer, Ando et al. recently found that methylation of miR-124a1-3 shows a similar pattern in the normal gastric mucosa from tumor and healthy subjects(18). We must mention that tissue specimens for normal colonic mucosa from CRC patients and healthy subjects were obtained from two different populations from Japan and Spain, respectively. Consequently, the differences in miR-137 methylation in these tissues could be attributed to other factors, such as ethnicity or other environmental factors which require further analysis to definitively establish the field defect associated with miR-137 methylation in the colon. Based on our findings for cancer-specificity, the high level of methylation in colonic adenomas, and the potential field defect feature, the methylation status of miR-137 may serve as a potential non-invasive biomarker for CRC.

Although several studies have demonstrated that miRNA expression profiles in CRC are significantly different than the normal colonic mucosa, it is unclear which specific cell types within the colon express various miRNAs. Elucidation of this aspect is essential to our understanding of the biological function of miRNAs in carcinogenesis, as these are known to have different roles in different cell types, and the same miRNA can act as a tumor suppressor or an oncogene depending on the tissue and cell compartment(2). *In situ* hybridization in FFPE tissues has been recently utilized for miRNA detection with great success for different cancers(19). We found that miR-137 is preferentially expressed in the epithelial cells of normal colonic mucosa, while no miR-137 expression was observed in any of the adenomatous polyps and CRC tissues. These findings are of significance, and are consistent with our gene-expression data which showed downregulation of miR-137 in CRC relative to normal mucosa.

Given the evidence that miR-137 is commonly silenced in CRC cell lines and CRC tissues due to promoter methylation, we performed functional studies to explore the potential tumor suppressor features of miR-137 *in vitro*. We discovered that the restoration of miR-137 expression in HCT116 and RKO cells, two cell lines with lower constitutive miR-137 expression, indeed resulted in a significant decrease in proliferation. Although further studies are needed, our results suggest that miR-137 may act as a tumor suppressor miRNA in CRC.

A critical and challenging step in understanding miRNA function is the identification of its gene targets. Lack of reliable and specific methods for target identification limits our understanding of the biological role of miRNAs. Computational methods, the most commonly used approach, are based on base-pairing between the miRNA seed region (first 2-8 bases of the mature miRNA) and the target, but suffer from specificity issues since predicted targets are usually in the hundreds or thousands, making it difficult to ascertain the authentic targets of a given miRNA. Whereas miRNAs were believed to act mainly through translational inhibition rather than mRNA cleavage, it is increasingly being realized that miRNAs may downregulate a much larger number of transcripts than previously appreciated(7,20,21). Thus, gene expression microarray analysis has been proposed as a useful strategy to identify physiologically relevant miRNA:mRNA interactions. In this study, candidate miR-137 targets were selected using a combination of bio-informatic and transcriptomic approaches. We used stringent criteria in order to decrease the false positivity rate, and identified 32 potential targets that were downregulated after miR-137 transfection at the mRNA level. These same gene targets were also predicted targets by at least 4 of the available computational-based prediction tools. It was encouraging to observe that our protein expression analysis revealed that three of the five selected genes also showed



corresponding downregulation of protein expression following miR-137 transfection, thus reinforcing the value of this strategy.

Interestingly, we found that *LSD1*, a histone demethylase, is a target of miR-137. *LSD1* is part of a new class of histone demethylating enzymes that, in addition to demethylating H3K4 and H3K9(22,23), are essential for the maintenance of global DNA methylation through the demethylation of a non-histone substrate, DNMT1, by increasing its stability(24). Since many human cancers show increased expression of DNMT1, it is plausible to speculate that *LSD1*, which is often upregulated in cancer cells, might be partly responsible for this epigenetic defect. Overexpression of *LSD1* has been documented in prostate cancer(22) and in neuroblastoma(25), where *LSD1* is involved in maintaining the undifferentiated phenotype and inhibition of its function inhibits tumor xenograft growth. In line with this argument, we found an inverse correlation between miR-137 and *LSD1* in CRC cell lines, and validated this functional interaction using luciferase experiments. Since *LSD1* seems to play a central role in the epigenetic machinery, and has a potential role in cancer therapy(26), future experiments will reveal additional roles of *LSD1* in CRC carcinogenesis, and its relationship to modulating the expression of miR-137.

In summary, this study first describes that miR-137 acts a tumor suppressor in the colon, is frequently silenced in CRC through promoter hypermethylation and its restoration inhibits cell proliferation *in vitro*. Since miR-137 methylation is an early-event in the colon, the potential use of miR-137 methylation as a CRC biomarker is very promising. We have identified multiple potential mRNA targets of miR-137 including *LSD1* in CRC, which provides novel evidence for the cross-talk between miRNAs and other components of the epigenetic machinery. These findings raise the possibility that in the future, miR-137 precursors may have potential therapeutic value in CRC patients.

## Supplementary Material

Refer to Web version on PubMed Central for supplementary material.

## Acknowledgments

Grant support: The present work was supported by grants R01 CA72851 and CA129286 from the National Cancer Institute, National Institutes of Health, and funds from the Baylor Research Institute to CRB and AG. FB was supported by a grant from Fundación Alfonso Martín Escudero and from Societat Catalana de Digestologia.

## References

1. Lu J, Getz G, Miska EA, Alvarez-Saavedra E, Lamb J, Peck D, et al. MicroRNA expression profiles classify human cancers. *Nature*. 2005; 435:834–8. [PubMed: 15944708]
2. Calin GA, Croce CM. MicroRNA signatures in human cancers. *Nat Rev Cancer*. 2006; 6:857–66. [PubMed: 17060945]
3. Lanza G, Ferracin M, Gafa R, Veronese A, Spizzo R, Pichiorri F, et al. mRNA/microRNA gene expression profile in microsatellite unstable colorectal cancer. *Mol Cancer*. 2007; 6:54. [PubMed: 17716371]
4. Schetter AJ, Leung SY, Sohn JJ, Zanetti KA, Bowman ED, Yanaihara N, et al. MicroRNA expression profiles associated with prognosis and therapeutic outcome in colon adenocarcinoma. *Jama*. 2008; 299:425–36. [PubMed: 18230780]
5. Doleshal M, Magotra AA, Choudhury B, Cannon BD, Labourier E, Szafranska AE. Evaluation and validation of total RNA extraction methods for microRNA expression analyses in formalin-fixed, paraffin-embedded tissues. *J Mol Diagn*. 2008; 10:203–11. [PubMed: 18403610]

6. Lujambio A, Ropero S, Ballestar E, Fraga MF, Cerrato C, Setien F, et al. Genetic unmasking of an epigenetically silenced microRNA in human cancer cells. *Cancer Res.* 2007; 67:1424–9. [PubMed: 17308079]
7. Toyota M, Suzuki H, Sasaki Y, Maruyama R, Imai K, Shinomura Y, et al. Epigenetic silencing of microRNA-34b/c and B-cell translocation gene 4 is associated with CpG island methylation in colorectal cancer. *Cancer Res.* 2008; 68:4123–32. [PubMed: 18519671]
8. Croce CM. Causes and consequences of microRNA dysregulation in cancer. *Nat Rev Genet.* 2009; 10:704–14. [PubMed: 19763153]
9. Bandres E, Agirre X, Bitarte N, Ramirez N, Zarate R, Roman-Gomez J, et al. Epigenetic regulation of microRNA expression in colorectal cancer. *Int J Cancer.* 2009; 125:2737–43. [PubMed: 19521961]
10. Grady WM, Parkin RK, Mitchell PS, Lee JH, Kim YH, Tsuchiya KD, et al. Epigenetic silencing of the intronic microRNA hsa-miR-342 and its host gene EVL in colorectal cancer. *Oncogene.* 2008; 27:3880–8. [PubMed: 18264139]
11. Lujambio A, Esteller M. CpG island hypermethylation of tumor suppressor microRNAs in human cancer. *Cell Cycle.* 2007; 6:1455–9. [PubMed: 17581274]
12. Bemis LT, Chen R, Amato CM, Classen EH, Robinson SE, Coffey DG, et al. MicroRNA-137 targets microphthalmia-associated transcription factor in melanoma cell lines. *Cancer Res.* 2008; 68:1362–8. [PubMed: 18316599]
13. Kozaki K, Imoto I, Mogi S, Omura K, Inazawa J. Exploration of tumor-suppressive microRNAs silenced by DNA hypermethylation in oral cancer. *Cancer Res.* 2008; 68:2094–105. [PubMed: 18381414]
14. Silber J, Lim DA, Petritsch C, Persson AI, Maunakea AK, Yu M, et al. miR-124 and miR-137 inhibit proliferation of glioblastoma multiforme cells and induce differentiation of brain tumor stem cells. *BMC Med.* 2008; 6:14. [PubMed: 18577219]
15. Xiao F, Zuo Z, Cai G, Kang S, Gao X, Li T. miRecords: an integrated resource for microRNA-target interactions. *Nucleic Acids Res.* 2009; 37:D105–10. [PubMed: 18996891]
16. Shen L, Kondo Y, Rosner GL, Xiao L, Hernandez NS, Vilaythong J, et al. MGMT promoter methylation and field defect in sporadic colorectal cancer. *J Natl Cancer Inst.* 2005; 97:1330–8. [PubMed: 16174854]
17. Ushijima T. Epigenetic field for cancerization. *J Biochem Mol Biol.* 2007; 40:142–50. [PubMed: 17394762]
18. Ando T, Yoshida T, Enomoto S, Asada K, Tatematsu M, Ichinose M, et al. DNA methylation of microRNA genes in gastric mucosae of gastric cancer patients: its possible involvement in the formation of epigenetic field defect. *Int J Cancer.* 2009; 124:2367–74. [PubMed: 19165869]
19. Schepeler T, Reinert JT, Ostefeld MS, Christensen LL, Silahtaroglu AN, Dyrskjot L, et al. Diagnostic and prognostic microRNAs in stage II colon cancer. *Cancer Res.* 2008; 68:6416–24. [PubMed: 18676867]
20. Lim LP, Lau NC, Garrett-Engele P, Grimson A, Schelter JM, Castle J, et al. Microarray analysis shows that some microRNAs downregulate large numbers of target mRNAs. *Nature.* 2005; 433:769–73. [PubMed: 15685193]
21. Chen X, Guo X, Zhang H, Xiang Y, Chen J, Yin Y, et al. Role of miR-143 targeting KRAS in colorectal tumorigenesis. *Oncogene.* 2009; 28:1385–92. [PubMed: 19137007]
22. Metzger E, Wissmann M, Yin N, Muller JM, Schneider R, Peters AH, et al. LSD1 demethylates repressive histone marks to promote androgen-receptor-dependent transcription. *Nature.* 2005; 437:436–9. [PubMed: 16079795]
23. Shi Y, Lan F, Matson C, Mulligan P, Whetstone JR, Cole PA, et al. Histone demethylation mediated by the nuclear amine oxidase homolog LSD1. *Cell.* 2004; 119:941–53. [PubMed: 15620353]
24. Wang J, Hevi S, Kurash JK, Lei H, Gay F, Bajko J, et al. The lysine demethylase LSD1 (KDM1) is required for maintenance of global DNA methylation. *Nat Genet.* 2009; 41:125–9. [PubMed: 19098913]

25. Schulte JH, Lim S, Schramm A, Friedrichs N, Koster J, Versteeg R, et al. Lysine-specific demethylase 1 is strongly expressed in poorly differentiated neuroblastoma: implications for therapy. *Cancer Res.* 2009; 69:2065–71. [PubMed: 19223552]
26. Huang Y, Stewart TM, Wu Y, Baylin SB, Marton LJ, Perkins B, et al. Novel oligoamine analogues inhibit lysine-specific demethylase 1 and induce reexpression of epigenetically silenced genes. *Clin Cancer Res.* 2009; 15:7217–28. [PubMed: 19934284]

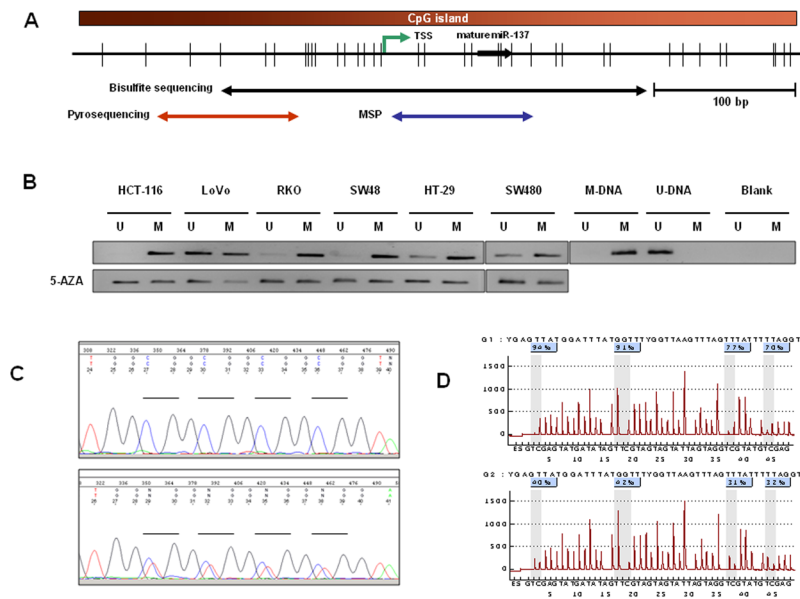


**Figure 1. Methylation analysis of miR-137 CpG island**

(A) Map of miR-137 CpG island, position of mature miR-137 and PCR products used for methylation analysis. Orange box, miR-137 CpG island; vertical tick marks, CpG sites; TSS, putative transcription start site. (B) MSP analyses for miR-137 methylation in CRC cell lines. U, unmethylated state; M, methylated state; U-DNA, normal lymphocytes; M-DNA, *in vitro* methylated DNA. Top, parental cell lines. Bottom, analysis after 5-AZA treatment. (C) Electropherogram corresponding to the bisulfite sequencing of 4 CpG sites in HCT116 cell line. Top panel, parental cell lines. Bottom panel, methylation analysis after 5-AZA treatment. Horizontal lines, CpG sites. (D) Results of bisulfite pyrosequencing of miR-137 in HCT116. Methylation percentages of 4 CpG sites (marked within gray vertical boxes) are indicated in the pyrogram. Top panel, parental cell lines with high levels of miR-137 methylation; Bottom panel, miR-137 demethylation after 5-AZA treatment.

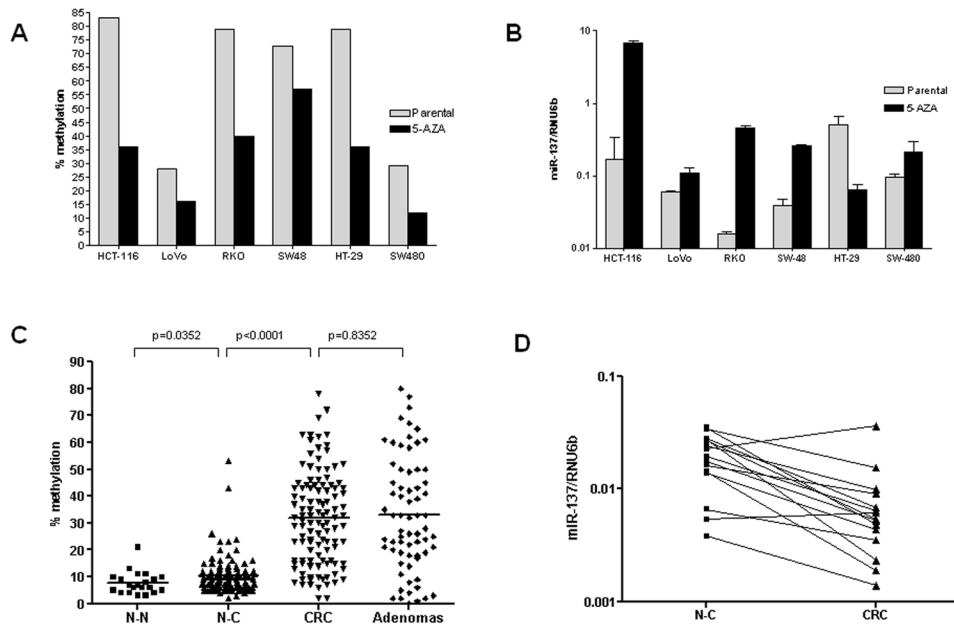


**Figure 2. Methylation and expression analyses of miR-137 CpG island in CRC cell lines and in CRC tissues**  
 (A) Bisulfite pyrosequencing results of miR-137 in 6 CRC cell lines. (B) TaqMan RT-PCR analysis of miR-137 expression in CRC cell lines. Results are expressed as  $2^{-\Delta\Delta Ct}$  (log10) and normalized to RNU6b. Error bars represent the standard deviation. (C) Bisulfite pyrosequencing results of miR-137 in colorectal tissues. N-N (n=21); N-C (n=111); CRC (n=113); adenomas (n=68). The black horizontal bar indicates mean methylation level. (D) TaqMan RT-PCR analysis of miR-137 expression in 15 paired CRC tissues and N-C. Results are expressed as  $2^{-\Delta Ct}$  and normalized to RNU6b.

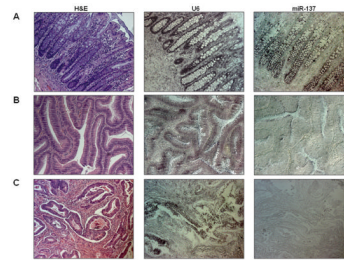


**Figure 3. *In situ* hybridization (ISH) analysis of miR-137 in normal colorectal mucosa and CRC** miR-137, positive control (U6) and negative control (no probe) ISH analysis were performed in normal colorectal mucosa (A) and a group of adenomas (B) and CRC (C). Staining for miR-137 was observed in the epithelium throughout the colonic crypt, with no staining of the stromal cells. However, miR-137 was not expressed in any of the neoplastic tissues evaluated. Hematoxylin-eosin (H&E) staining of the corresponding tissues is shown.

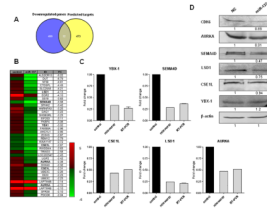


**Figure 4. Identification of potential targets of miR-137 in CRC**

(A) The Venn diagram represents the downregulated genes ( $\geq 2$  fold-change) observed in the gene expression microarray analysis after transfection of miR-137 precursor (in blue), and the predicted targets generated by the *in silico* prediction tool miRecords (in yellow). (B) The list of genes identified using the mentioned strategy. The expression intensity of each mRNA varies from red (above the average) to green (below the average). ID, gene name; FC, fold-change. (C) Comparison between the qRT-PCR and microarray results. For each gene, the variation in expression compared to control is represented as average fold-change for both the microarray and the qRT-PCR analysis (error bars represent the standard deviation). (D) Western-blot analysis of potential miR-137 targets. Densitometric analysis of protein expression is shown below each blot, in relation to NC and normalized to  $\beta$ -actin expression.

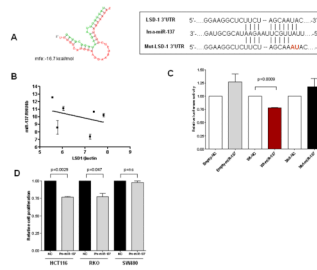


**Figure 5. Interaction between miR-137 and *LSD1* and tumor suppressor features of miR-137**  
 (A) The predicted hybridization of miR-137 (green) with the 3'UTR region of *LSD1* mRNA (red) using RNAhybrid software. The minimum free energy (mfe) required for RNA hybridization is shown. The conserved predicted binding site of miR-137 with the 3'UTR region of *LSD1* mRNA is also represented. The mutated binding site used for the luciferase assay is shown in red. (B) Correlation between miR-137 expression and *LSD1* mRNA levels across a panel of 6 CRC cell lines. Results are expressed as  $2^{-\Delta C_t}$ . RNU6b and  $\beta$ -actin were used for normalization, respectively. Error bars represent the standard deviation. (C) Direct recognition of *LSD1* mRNA 3'UTR by miR-137. Luciferase assay of HCT116 cells transfected with firefly luciferase constructs containing *LSD1*-mut or *LSD1*-wt. The parental luciferase plasmid (empty) was also transfected as a control.  $\beta$ -galactosidase activity was calculated for normalization. Error bars represent standard deviation. (D) Effect of miR-137 on cell proliferation (BrdU assay). Error bars represent standard deviation.



**Table 1**

Clinico-pathological features of colorectal cancer patients analyzed for miR-137 methylation.

	Whole cohort (n=113)	miR-137 unmethylated (n=21)	miR-137 methylated (n=92)	p-value
Age, mean (SD)	64.88 (11.17)	60 (14.1)	66 (10)	<b>0.024</b> <sup>†</sup>
Age >65, n (%)	59 (52.2)	9 (42.9)	50 (54.3)	0.342 <sup>‡</sup>
Female, n (%)	47 (41.6)	7 (33.3)	40 (43.5)	0.395 <sup>‡</sup>
Proximal location, n (%) <sup>*</sup>	32 (28.3)	7 (35)	25 (27.2)	0.483 <sup>‡</sup>
MSI, n (%)	1 (0.9)	0 (0)	1 (1.1)	1 <sup>‡</sup>
KRAS mutation, n (%)	37 (32.7)	3 (14.3)	34 (37)	<b>0.046</b> <sup>‡</sup>
BRAF mutation, n (%)	4 (3.5)	0 (0)	4 (4.3)	1 <sup>‡</sup>
Poorly differentiated adenocarcinoma, n (%) <sup>*</sup>	9 (8)	3 (15)	6 (6.5)	0.2 <sup>‡</sup>
Mucinous adenocarcinoma, n (%) <sup>*</sup>	5 (4.5)	3 (15)	2 (2.2)	<b>0.039</b> <sup>‡</sup>
TNM <sup>*</sup>				
I	14 (12.5)	3 (15)	11 (12)	0.713 <sup>‡</sup>
II	34 (30.4)	5 (25)	29 (31.5)	0.565 <sup>‡</sup>
III	43 (38.4)	5 (25)	38 (41.3)	0.174 <sup>‡</sup>
IV	21 (18.8)	7 (35)	14 (15.2)	0.057 <sup>‡</sup>

<sup>†</sup> Evaluated with t-Student's test.<sup>‡</sup> Evaluated with Chi-square test or the Fisher's exact test<sup>\*</sup> Results referred to 112 patients

SD, standard deviation; MSI: microsatellite instability;